



HAL
open science

Na⁺ Sensitivity of the KAT2-Like Channel Is a Common Feature of Cucurbits and Depends on the S5-P-S6 Segment

Li-Min Wang, Li-Na Zhao, Iftikhar Hussain Shah, Dora Cano Ramirez, Martin Boeglin, Anne-Aliénor Véry, Hervé Sentenac, Yi-Dong Zhang

► **To cite this version:**

Li-Min Wang, Li-Na Zhao, Iftikhar Hussain Shah, Dora Cano Ramirez, Martin Boeglin, et al.. Na⁺ Sensitivity of the KAT2-Like Channel Is a Common Feature of Cucurbits and Depends on the S5-P-S6 Segment. *Plant and Cell Physiology*, 2022, 63 (2), pp.279-289. 10.1093/pcp/pcab170 . hal-03713441

HAL Id: hal-03713441

<https://hal.inrae.fr/hal-03713441>

Submitted on 9 Aug 2022

HAL is a multi-disciplinary open access archive for the deposit and dissemination of scientific research documents, whether they are published or not. The documents may come from teaching and research institutions in France or abroad, or from public or private research centers.

L'archive ouverte pluridisciplinaire **HAL**, est destinée au dépôt et à la diffusion de documents scientifiques de niveau recherche, publiés ou non, émanant des établissements d'enseignement et de recherche français ou étrangers, des laboratoires publics ou privés.



Distributed under a Creative Commons Attribution 4.0 International License

Cover Page

Running title: KAT2-like channels from Cucurbits sensitive to Na⁺

Na⁺ sensitivity of the KAT2-like channel is a common feature of Cucurbits and depends on the S5-P-S6 segment

Corresponding author: Yi-Dong Zhang

School of Agriculture and Biology, Shanghai Jiao Tong University, 800 Dongchuan Road, Shanghai, 200240, People's Republic of China.

Tel & Fax: 86-21-34206973,

E-mail: zhyd@sjtu.edu.cn

Subject areas: membrane and transport

Number of figures: 6

Number of supplementary tables: 1

Number of supplementary figures: 5

ACCEPTED MANUSCRIPT

Running title: KAT2-like channels from Cucurbits sensitive to Na⁺

Na⁺ sensitivity of the KAT2-like channel is a common feature of Cucurbits and depends on the S5-P-S6 segment

Li-Min Wang^{1,2,3,#}, Li-Na Zhao^{1,#}, Iftikhar Hussain Shah¹, Dora Cano Ramirez⁴, Martin Boeglin², Anne-Aliénor Véry², Hervé Sentenac², Yi-Dong Zhang^{1,2*}

¹ School of Agriculture and Biology, Shanghai Jiao Tong University, 800 Dongchuan Road, Shanghai, 200240, People's Republic of China

² Biochimie et Physiologie Moléculaires des Plantes, Univ Montpellier, CNRS, INRAE, Institut Agro, 34060 Montpellier Cedex 2, France

³ Present address: Department of Plant and Microbial Biology, University of Zurich, Zollikerstrasse 107, 8008 Zurich, Switzerland

⁴ Department of Plant Sciences, University of Cambridge, Downing Street, Cambridge CB2 3EA, United Kingdom

[#] These authors contributed equally to this work.

* Corresponding author:

Yi-Dong Zhang, Tel: 86-21-34206973, E-mail: zhyd@sjtu.edu.cn;

Abstract

Inhibition of Shaker K⁺ channel activity by external Na⁺ was previously reported in the melon (*Cucumis melo* L.) inwardly-rectifying K⁺ channel MIRK and was hypothesized to contribute to salt tolerance. In this study, two inward Shaker K⁺ channels, CsKAT2 from cucumber (*Cucumis sativus*) and CIKAT2 from watermelon (*Citrullus lanatus*) were identified and characterized in *Xenopus* oocytes. Both channels were inwardly-rectifying K⁺ channels with higher permeability to potassium than other monovalent cations and more active when external pH was acidic. Similarly to MIRK, their activity displayed an inhibition by external Na⁺, thus suggesting a common feature in Cucurbitaceae (*Cucumis* spp., *Citrullus* spp.). CsKAT2 and CIKAT2 are highly expressed in guard cells. After 24 h of plant treatment with 100 mM NaCl, the three *KAT2*-like genes were significantly down-regulated in leaves and guard cells. Reciprocal chimeras were obtained between *MIRK* and Na⁺-insensitive *AtKAT2* cDNAs. The chimera where the *MIRK* S5-P-S6 segment was replaced by that from *AtKAT2* no longer showed Na⁺ sensitivity, while the inverse chimera gained Na⁺ sensitivity. These results provide evidence that the molecular basis of the channel blockage by Na⁺ is located in the S5-P-S6 region. Comparison of the electrostatic property in the S5-P-S6 region in *AtKAT2* and *MIRK* revealed four key amino-acid residues potentially governing Na⁺ sensitivity.

Key words: Chimera channel, Cucurbitaceae, Electrophysiology, Inhibition by Na⁺, *KAT2*-like channels, Structure-function analysis

Accession numbers: The nucleotide sequences of *CsKAT2* and *CIKAT2* reported in this article have been submitted to GenBank under accession numbers MF447463 and MF447464.

Introduction

Salt stress hinders plant development and leads to wholesale reduction of agricultural productivity. For plants, the sodium ion is harmful since high levels of Na^+ in the cytoplasm, in contrast to K^+ , can disrupt various enzymatic functions (Benito et al. 2014). Due to physicochemical similarities between Na^+ and K^+ , excess Na^+ will tend to substitute K^+ for Na^+ at binding sites and impair cellular biochemistry (Bhandal and Malik 1988; Serrano 1996; Tester and Davenport 2003; Maathuis 2006). Therefore, maintaining a low concentration of Na^+ or high K^+/Na^+ ratio in the cytosol of plant cells through regulation of K^+ and/or Na^+ transporters or channels (Kronzucker and Britto, 2011; Benito et al. 2014; Demidchik 2014) is essential for the adaptation of plants to saline conditions (Asch et al. 2000; Tester and Davenport 2003).

Regarding K^+ channels, particularly in the Shaker family, regulation by saline conditions has mostly been studied at the transcriptional level. The abundance of Shaker family transcripts differs greatly in response to saline stress (Su et al. 2001; Gollack et al. 2003; Pilot et al. 2003a; Zhang et al. 2006; Obata et al. 2007; Escalante-Pérez et al. 2009). For instance, *Arabidopsis AtKC1*, a general modulator of inward Shaker channel activity (Jeanguenin et al. 2011), its transcript accumulation was strongly induced in leaves under salt stress, suggesting a key role of the protein in adaption to saline conditions (Pilot et al. 2003a). In barley, *HvAKT1* in the elongation zone of leaves was also induced by sodium, contributing to the maintenance of K^+ concentration in mesophyll cells under salinity (Boscardi et al. 2009). Also in the halophyte *S. salsa*, up-regulation of *SsAKT1* expression was observed under saline conditions, which may contribute to mediating significant K^+ uptake in roots from the external medium (Duan et al. 2015). Such regulation was reported for other plant species, like *BrKCT2* from *Brassica rapa* ssp. *Pekinensis* (Zhang et al. 2006), *BnGORK* from *Brassica napus* (Chakraborty et al. 2016), and *PtKPT1* in the bark of grey poplar (Escalante-Pérez et al. 2009). In contrast, the transcript levels of *McMKT1* from the common ice plant (*Mesembryanthemum crystallinum*), *OsAKT1* from rice (*Oryza sativa* L. ssp. *japonica* cv. *Nihonmasari*), and *AtAKT1* from *Arabidopsis thaliana* have been shown to be down-regulated in the presence of excessive Na^+ (Su et al. 2001; Fuchs et al. 2005; Kaddour et al. 2009). However, *PutAKT1* transcript levels from *Puccinellia tenuiflora* seem to be unaffected by salt stress (Ardie et al. 2010).

The activity of plant K^+ channels is also regulated by protein kinases and phosphatases (Zhu 2003). Little is known about the effect of Na^+ on the activity of plant K^+ channels (Zhang et al. 2011).

Electrophysiological analyses on guard-cell protoplasts from a salt-tolerant *Aster* species revealed that an increase in cytosolic Na⁺ concentration in guard cells caused a delayed and dramatic deactivation of K⁺ inward conductance (Véry et al. 1998). Also, an irreversible blockage/inactivation of inward rectifying K⁺ currents by low external Na⁺ was observed in *Avena sativa* mesophyll cells (Kourie & Goldsmith 1992). More recently, a direct effect of external Na⁺ on the activity of the Shaker inward K⁺ channel MIRK (belonging to KAT subgroup) from melon (*Cucumis melo*) has been reported (Zhang et al. 2011). In *Xenopus* oocytes, external Na⁺ downregulated both inward and outward MIRK currents in a voltage-independent manner, suggesting a blocking site in the external mouth of the channel. The addition of 100 mM Na⁺ at low (submillimolar) external K⁺ concentrations completely suppressed the MIRK-like K⁺ channel activity. The molecular site(s) of the inhibition by Na⁺ in the MIRK channel was speculated to be located in the S5-P-S6 (Transmembrane segment 5-Pore-Transmembrane segment 6) region (Zhang et al. 2011). Three site-specific mutants (S232KQ-PRK, N241-Y and L252-R) within the S5-P-S6 region were obtained and studied using electrophysiological analyses to identify the molecular site(s) of Na⁺ inhibition in MIRK. The S232KQ-PRK and N241-Y, but not L252-R, mutant channels had a reduced Na⁺ inhibition rate. Among these three mutants, N241-Y had the strongest reduction of Na⁺ inhibition rate. However, as the Na⁺ effect was not completely abolished, it is likely that MIRK sensitivity to Na⁺ is determined by more than one residue (Wang et al. 2011). The molecular basis of sodium blockage in MIRK thus needs to be further explored.

In the Cucurbitaceae family, besides melon, cucumber (*Cucumis sativus*) and watermelon (*Citrullus lanatus*) are two other common kinds of vegetable crops cultivated worldwide. To date, no K⁺ channels from these two plants have ever been documented. In this study, two Shaker genes that are homologous to *KAT2* were isolated from *Cucumis sativus* L. and *Citrullus lanatus* L., named *CsKAT2* and *CIKAT2* respectively. The electrical properties of these two K⁺ channels were studied in *Xenopus* oocytes, in particular the regulation by Na⁺ of these two Shaker K⁺ channels, with the aim of determining whether inhibition by Na⁺ is ubiquitous in the KAT-type Shaker channels from Cucurbitaceae. The question of the molecular location of the sodium blockage in MIRK channel was also further analyzed in this study.

Results

Identification of the *CsKAT2* and *CIKAT2* Shaker channel genes

The Shaker Channel genes *CsKAT2* (GenBank accession number MF447463) and *CIKAT2* (GenBank accession number MF447464) were obtained by PCR. The open reading frame (ORF) of *CsKAT2* was 2100 bp long encoding a 700 amino acid polypeptide, and *CIKAT2* contained 2061 bp encoding a 687 amino acid polypeptide. Results of BLAST revealed a high degree of homology between amino acid sequences of *CsKAT2*, *CIKAT2* and *MIRK*. *CsKAT2* and *CIKAT2* shared 91% and 90% amino acid identity with *MIRK*, respectively. These three channels shared, respectively, 62%, 61% and 62% amino acid identity with *KAT2* from *Arabidopsis*. They all displayed high sequence conservation in the pore domain with the putative K⁺ transport motif (TLETTTGYGD), which is common to the other Shaker channel genes (Fig S1). The phylogenetic tree of Shaker channel proteins confirmed that *CsKAT2*, *CIKAT2* and *MIRK* proteins were genetically close and that all belong to the KAT-like channel subgroup (Fig 1).

Electrophysiological characterization of *CsKAT2* and *CIKAT2* channels in *Xenopus* oocytes

In contrast to *Xenopus* oocytes injected with H₂O (Fig 2A), the oocytes expressing *CsKAT2* and *CIKAT2* elicited the classical inwardly-rectifying currents, from a voltage threshold around -105 mV (*CsKAT2*) or -120 mV (*CIKAT2*) in 10 mM external K⁺ (Fig 2B, C). When K-glutamate concentration (1, 3, 10, or 100 mM, at pH 5.5) increased in the external solution, the magnitude of whole-oocyte steady-state *CsKAT2* and *CIKAT2* inward currents was increased at the same voltage. As expected for an inward K⁺ channel, the increase of external K⁺ concentration also positively shifted the reversal potential (E_{rev}) of currents. A 10-fold change in the external K⁺ resulted in 50 mV and 53 mV differences in E_{rev} for *CsKAT2* and *CIKAT2*, respectively, which was close to the theoretical behavior of a pure K⁺ channel (Fig 2D, E). Half-saturation of *CsKAT2* and *CIKAT2* conductance was observed at around 7 mM and 9 mM of external K⁺, respectively (Fig 2F). The affinity to K⁺ of both channels was thus close to that reported for *MIRK* channel ($K_{1/2}$ =11 mM; Zhang et al. 2011) and was in the lowest range of most other plant inward Shaker channels (Very et al. 2014). Analysis of *CsKAT2* and *CIKAT2* voltage sensitivity unveiled that their gating voltage-dependency was unaffected by external K⁺ (Fig 2G). When successively replacing K⁺ in the bath solution with the same concentration of Rb⁺, NH₄⁺, Li⁺ or Na⁺, current-voltage relationships indicated that *CsKAT2* and *CIKAT2* channels were

mostly permeable to K^+ , and a lesser extent to Rb^+ and NH_4^+ (Fig 2H). P_{Rb}/P_K and P_{NH_4}/P_K of CsKAT2 calculated from the reversal potential analyses were 0.30 ± 0.02 (n=9) and 0.05 ± 0.003 (n=9), respectively. For ClKAT2, they were 0.25 ± 0.02 (n=11) and 0.04 ± 0.001 (n=11). Both channels are not significantly permeable to Li^+ or Na^+ (Fig 2H). Like other KAT2-type channels, CsKAT2 and ClKAT2 were regulated by the external pH (Pilot et al. 2003b; Véry et al. 2014). The acidification, specifically from pH 7.5 to 6, led to an increase of inward CsKAT2 and ClKAT2 currents (Fig 2I).

CsKAT2 and ClKAT2 currents were inhibited by external Na^+ , as MIRC currents

Similar to the MIRC currents in *Xenopus* oocytes, CsKAT2 and ClKAT2 currents recorded in the solution containing 1 mM K^+ and 99 mM Na^+ were clearly smaller than those in the solution with same concentration of K^+ but with 99 mM Li^+ (Fig 3A, B; upper panels). The “tail” currents (transient outward currents recorded upon channel deactivation when the membrane polarization was back to weak value) of both channels were inhibited as well in the presence of external Na^+ (Fig 3A, B; lower panels). Current inhibition by Na^+ in either inward or outward directions was not dependent on voltage. Mean I-V relationship led to the same conclusion (Fig 3D, E). Like in MIRC, both channels were no longer blocked by Na^+ when high K^+ concentration (≥ 10 mM) was present in the bath (Fig S2). AtKAT2 from *Arabidopsis* was expressed in oocytes in order to make the comparison under the same recording conditions. The AtKAT2 currents were not sensitive to external Na^+ (Fig 3C, F). Consistently, at -155 mV, the extent of Na^+ inhibition in CsKAT2, ClKAT2 and MIRC was high, which contrasted to KAT2 from *Arabidopsis*. No significant difference in the degree of inhibition was found among the three Cucurbitaceae-family channels (Fig 3G).

KAT2-like channel genes in cucurbits were significantly downregulated under NaCl treatment

Quantitative RT-PCR results provided evidence that *CsKAT2* and *ClKAT2*, like *MIRC* (Zhang et al., 2011), are primarily expressed in leaves, particularly in guard cells (Fig 4A). To determine whether the expression of *KAT2-like* genes was modulated by external Na^+ treatments, total RNA was collected from leaves and guard cells of plants exposed to salt stress for 24 h using 100 mM NaCl-supplemented growth solution. As shown in Fig 4B, *KAT2-like* genes were slightly affected by the salt stress in whole leaves or guard cells. Salt stress tended to down regulate the *KAT2-type* genes, the decrease being significant in all of three genes in the whole leaf and guard cells (Fig 4B).

Inhibition by Na⁺ was abolished in a chimeric MIRK channel harboring AtKAT2 S5-P-S6 domain, but re-appeared in the reciprocal chimera

A molecular determinant of the inhibition by Na⁺ in the MIRK channel could be suspected to be located in the S5-P-S6 region (which constitutes the channel pore), especially in the S5-P linker (Zhang et al. 2011). The S5-P-S6 region harbored eighteen amino acid differences between AtKAT2 and MIRK (and the two other KAT-type channels from Cucurbitaceae; Fig 5 and S1). To confirm the hypothesis that the molecular site of Na⁺ inhibition in MIRK is located in this area, we replaced the whole segment of the S5-P-S6 region of *MIRK* containing the sequence of the eighteen amino acids different from *AtKAT2* (i.e. amino acids between the two inverted triangles in Fig 5A) by the corresponding position in *AtKAT2* (Fig 5A). The chimera in *MIRK* cDNA was named *MIRK-By-ΔAtKAT2*.

Expressed in *Xenopus* oocytes, *MIRK-By-ΔAtKAT2* displayed classical inwardly-rectifying currents in K⁺-containing solutions (Fig 5B and Fig S3 A). The activation threshold of *MIRK-By-ΔAtKAT2* channel was about -105 mV, which was close to that of MIRK (-110 mV) in K⁺-containing solutions (Fig S3 B; Zhang et al. 2011). The kinetics of current activation and deactivation appeared similar in MIRK and *MIRK-By-ΔAtKAT2* (Fig 5B and S3 A; Zhang et al. 2011). The potassium sensitivity of *MIRK-By-ΔAtKAT2* currents, tested at three different potassium concentrations (1, 10 and 100 mM) was very similar to that reported for MIRK (Fig S3 B; Zhang et al. 2011), which indicated that the affinity to K⁺ was not significantly modified in the chimera. The reversal potential of *MIRK-By-ΔAtKAT2* current shifted toward a more positive value as the K⁺ concentration increased, with a 56 mV difference per 10-fold change in external K⁺ concentration (Fig S3 C). This was very close to the theoretical behavior of a pure K⁺ channel, as previously reported for MIRK (Zhang et al. 2011). Thus, the above analyses proved that the substitution of amino acids in the region forming the channel pore with AtKAT2 did not change the basic properties of MIRK. Thereafter, *MIRK-By-ΔAtKAT2* currents were investigated at 1 mM K⁺, either in the presence of Li⁺ (99 mM) or Na⁺ (99 mM), to test the sensitivity to Na⁺. Comparing the representative current traces between these two conditions, the current activation and deactivation magnitudes were similar (Fig 5B). Statistical analyses confirmed that there was no significant difference in the inward currents between the two conditions. This observation was verified in three independent experiments (Fig 5C). Therefore, we concluded that the inhibition by Na⁺ was abolished in the *MIRK-By-ΔAtKAT2* channel.

To confirm the above result, we created the reciprocal chimera, termed *AtKAT2-By-ΔMIRK*, by substituting the whole segment of the S5-P-S6 region of *AtKAT2* for the corresponding residues from *MIRK*. The same solutions (1 mM K⁺, either in the presence of Li⁺ (99 mM) or Na⁺ (99 mM)) were used to test the Na⁺ sensitivity. Expressed in oocytes, *AtKAT2-By-ΔMIRK* is capable of inducing the typical inwardly-rectifying currents in both solutions. The inward currents in K1Li99 condition were twice as large than that in K1Na99. The same observation was found at the “tail” currents (Fig 5D). Mean I/V plots (Fig 5E) confirmed that the inhibition by external Na⁺ re-appeared in *AtKAT2-By-ΔMIRK* channel. In summary, we conclude that the S5-P-S6 region is important for determining Na⁺ sensitivity in the MIRK channel.

Discussion

Identification of two novel K⁺ Shaker channels from Cucurbits

The Cucurbitaceae family includes more than 700 species worldwide and many of them are very agronomically important (Jeffrey 1980). For example, watermelon and cucumber are extensively cultivated in China, accounting for 60% of the cultivated areas in the world (<http://faostat.fao.org/>, 2018). Studies over the last few decades have focused on the physiological importance of K⁺ nutrition on the growth, yield and fruit quality of these two vegetable crops (Gislerød and Adams 1983; Altunlu et al. 1997; Kaya et al. 2001), but few concerned the molecular identity of K⁺ acquisition and transport pathways. In this study, two more Shaker channel genes, *CsKAT2* and *CIKAT2* from cucumber and watermelon, respectively, were cloned and studied, reinforcing the information on the Shaker family from the plant kingdom.

Based on the phylogenetic analyses, the closest homolog of *CsKAT2* and *CIKAT2* among reported Shaker channels is *MIRK*, also from the Cucurbitaceae family, melon (Fig 1). The three channels have more than 90% conserved amino acid identity. Electrophysiological results obtained in the heterologous system *Xenopus* oocytes showed that *CsKAT2* and *CIKAT2* shared a number of functional properties with *MIRK* as well as other homologs from the KAT subfamily, however there were a few differences in quantitative parameters (Fig 2). For instance, *CsKAT2* and *CIKAT2*, like *MIRK* and other KAT2-type channels, share similar gating properties. However, among *CsKAT2*, *CIKAT2*, *MIRK* and *AtKAT2*, *MIRK* shows the highest equivalent gating charge ($z=3$, 2-folds higher than that of *CsKAT2*) and also the most negative half activation potential (> 30 mV more negative than

that of AtKAT2) (Fig 2G, Pilot et al. 2003b; Zhang et al. 2011). The affinity of CsKAT2, ClKAT2 and MIRK to external K^+ are very similar (Fig 2F; Zhang et al. 2011), but more than 2-fold higher than that of AtKAT2 from *Arabidopsis* (Jeanguenin et al. 2011) and about 4-fold higher than that of ZmK2.1 from maize (Su et al. 2005). Comparison of CsKAT2, ClKAT2 and MIRK cationic selectivity to different monovalent cations resulted in a similar sequence: for conductances, $K^+ > Rb^+ \approx NH_4^+ \gg Li^+ \approx Na^+$ (Fig 2H, Zhang et al. 2011). Like most other channels from the KAT subfamily (Hoth and Hedrich 1999; Zhang et al. 2011; Yang et al. 2015), CsKAT2 and ClKAT2 were activated by acidic external pH (Fig 2I).

KAT2-type channels inhibited by external Na^+ : a common feature in cucurbits?

MIRK from melon was the first cloned plant K^+ channel reported whose activity was directly inhibited by external Na^+ (Zhang et al. 2011). In this study, we reported two other Shaker K^+ channels from cucumber and watermelon whose activities were also blocked by external Na^+ (Fig 3). All three channels are from the gourd species, belonging to Cucurbitaceae. Is this inhibition of channel activity by external Na^+ a common feature among KAT2-type channels from the whole Cucurbitaceae family? Cloning other KAT2-type channels from more distant species in the Cucurbitaceae family and study of their electrical properties with respect to external Na^+ effect would be very informative regarding the above question.

Detailed analyses of the Na^+ effect on CsKAT2 and ClKAT2 activity revealed three common features with MIRK: i) the inhibition of inward currents by external Na^+ was immediately observed when Na^+ was added into the bath and quickly reversed upon Na^+ removal; ii) the inhibition by external Na^+ presented no voltage dependency; iii) Na^+ was not permeant through these channels (Fig 2H and 3 D, E). Given the above consistency, it is highly likely that the inhibitory mechanism of CsKAT2 and ClKAT2 channels by Na^+ and the molecular regions underpinning this phenomenon are the same as for MIRK.

The inhibitory effect of Na^+ on MIRK inward activity was completely abolished by replacing the S5-P-S6 segment of MIRK with the corresponding sequence from *Arabidopsis* AtKAT2 and was recovered in the reciprocal chimera (Fig 5), indicating that S5-P-S6 is crucial for MIRK sensitivity to Na^+ . The three channels from Cucurbitaceae display the same level of inhibition by Na^+ (Fig 3G) and share 18 amino acid differences with AtKAT2 in this region (Fig S1). Among these amino acids, 2 are

located at the base of the S5 segment and 13 in the external S5-P linker, known to constitute the external mouth of the channel pore. Since the level of inhibition by external Na^+ is not dependent on voltage and is immediately reversed upon Na^+ removal, it is likely that the molecular site of the inhibition within the S5-P-S6 region is in the S5-P linker (Zhang et al. 2011). To identify key amino acid residues, we used MIRROR for homology modelling and compared it to AtKAT2.

Homology modeling and electrostatic comparison identify four key amino-acid residues in MIRROR that may account for Na^+ sensitivity

Based on the Cryo-EM structure of AtKAT1 (Clark et al. 2020), we built homology models of AtKAT2 and MIRROR. Similar to AtKAT1, both AtKAT2 and MIRROR assemble as a tetrameric channel with a 4-fold symmetry and with the pore domain (in Red) at the center (Fig 6A). Electrostatic interactions in the MIRROR and AtKAT2 models were mapped. As seen, the pore entrances are predominantly negatively charged (white arrow; Fig 6B). The amino acid residues from the end part of S5 and S5-P linker (green line surrounded, Fig 6B) were located around the mouth of the pore entrance. In this region, MIRROR had less positively charged amino acids than AtKAT2 (Fig S1), globally providing a more negative charge environment (Fig 6B, C). In this case, there is a higher possibility of favoring binding of sodium ions in MIRROR than in AtKAT2. Further comparison of the electrostatic potential distribution on surface for residues N222 to S260 in MIRROR and the corresponding residues from A216 to S254 in AtKAT2 was carried out (Fig S4). Of 15 residues, four amino-acid residues, P230, N241, E247 and N251 in MIRROR had more negative surface charge than those corresponding residues, H224, Y235, T241 and S245 in AtKAT2 (Fig 6D and Fig S4), which may account for Na^+ sensitivity. Of these, the N241-Y mutation has been shown to induce a lower Na^+ inhibition rate (Wang et al. 2011), and we also tested MIRROR mutated at 6 sites together (SKQ232-PRK, N241-Y, L252-R and D283-F). The sensitivity to Na^+ in this sextuple mutant was significantly reduced but still not completely abolished (Fig S5). Given the modeling analysis and the oocyte results, MIRROR sensitivity to Na^+ seems to be governed by several residues. Of note, glutamic acid (Glu; E) in MIRROR and CsKAT2 or aspartic acid (Asp; D) in AtKAT2 (FigS1; Green triangle) is negatively charged and the ability for Na^+ binding is prevalent (Handling, et al. 2018). Further analyses on the channels including D/E mutation would be helpful to better understand the common Na^+ sensitivity.

Possible role of KAT2 type channels from cucurbits in response to salt stress

K⁺ channels in plants play important roles in K⁺ absorption and transport, particularly in regulating cellular homeostasis under abiotic stress (Pilot et al. 2003a; Maathuis 2005). Shaker K⁺ channels from several plant species were found at the transcriptional level to be affected (down- or up-regulated) by salt stress (Su et al. 2001; Pilot et al. 2003a; Fuchs et al. 2005; Zhang et al. 2006; Escalante-Pérez et al. 2009; Kaddour et al. 2009; Jeanguenin et al. 2011; Chakraborty et al. 2012; Duan et al. 2015). In this study, the expression of *CsKAT2*, *CIKAT2* and *MIRK* was down regulated in response to 100 mM NaCl (Fig 4), as observed for that of the Shaker AKT subgroup (Véry et al. 2014) *McMKT1* in *Mesembryanthemum crystallinum* (Su et al. 2001) and *OsAKT1* (Gollack et al. 2003; Fuchs et al. 2005). The transcriptional downregulation of the three cucurbit KAT-type channels is consistent with the inhibition of these channels by external Na⁺ (Fig 3G), suggesting that Na⁺ regulation has an important role in response to salt stress in these species.

The Shaker KAT group has been characterized by expression of its members in guard cells (Véry et al., 2014). Quantitative RT-PCR showed that all three *KAT2* type channels from Cucurbitaceae family were mostly expressed in guard cells (Fig 4), supporting the fact that all three channels belong to the KAT group (Pilot et al. 2003b).

The inhibition of KAT2-like channel activities by external Na⁺ occurred when K⁺ was in the range 0.1-1 mM and Na⁺ in the range 10-100 mM (Fig 3 and Zhang et al., 2011). This can be predicted to be physiologically relevant in guard cells upon salt stress. Very substantial reduction of inward K⁺ transport across guard cells is expected with the combined transcriptional and channel activity inhibitions, in the presence of 100 mM Na⁺ and ≤1 mM K⁺ in the guard cell apoplast. It should also be noted that at a low K⁺ concentration like 0.1 mM, an even higher suppression of channel activity occurred in the presence of 100 mM Na⁺, which reached 86% and 94% for *CsKAT2* and *CIKAT2* respectively (data not shown). Inhibiting the expression and activity of guard cell inward channels likely contributes to reduced stomatal aperture (Lebaudy et al. 2008), an adaptive response to the osmotic stress and to excess salt arrival to the shoot caused by salt stress (Robinson et al. 1997; Munns and Tester 2008). Our previous experiments showed high correlation between stomatal movement and *MIRK* transcription level (Wang et al. 2013). Thus, our results suggest that KAT-like K⁺ channels of cucurbits (gourds at least) have special characteristics (intrinsic functional properties and expression regulation), which may contribute to salt stress adaptation.

Materials and methods

Genes cloning and phylogenetic analyses

Total leaf RNA (~ 5 µg) of cucumber (*Cucumis sativus*) and watermelon (*Citrullus lanatus*) was used to synthesize the first strand cDNA according to the manual of the Thermo First Strand cDNA synthesis Kit (USA). The primers CsKAT2-F 5'-ATGCGATGCTCTTGTGTACAA-3' and CsKAT2-R 5'-TCATTGGAGACCACAATTTGA-3' were used for obtaining *CsKAT2* full length (coding sequence), and CIKAT2-F 5'-ATGCGATGTTCTTACTGTACAA-3'; CIKAT2-R 5'-TCATTG(A/G)AGACCACAATTT(C/G)A-3' for *CIKAT2* (coding sequence). With the first strand cDNA as the template, PCR amplification was performed for 35 cycles (94°C for 45 s, 62°C for 40 s, and 72°C for 100 s) followed by a final extension step of 8 min at 72°C. The amplified PCR product was gel purified and cloned into pGEM-T Easy plasmid (Promega, USA). Similarity-based analyses were carried out using BLAST on NCBI (<http://www.ncbi.nlm.nih.gov/BLAST/>). The phylogenetic tree was constructed using the full length amino acid sequences of plant inwardly-rectifying potassium channels with Geneious 7.1 Pro™ Phylogenetics analysis (<http://www.geneious.com>) using the Neighbor-joining method.

Construction of the K⁺ channel gene chimera *MIRK-By-ΔAtKAT2* and *AtKAT2-By-ΔMIRK*

A chimeric cDNA of *MIRK* channel subunit in which *AtKAT2* S5-P-S6 region replaced the corresponding *MIRK* sequence, *MIRK-By-ΔAtKAT2* was obtained by a series of PCR programs. Based on sequence analysis of the S5-P-S6 region of the two Shaker channels *AtKAT2* and *MIRK* (Fig. S1), three pairs of primers were designed (Table S1). The first PCR product *MIRK-S1* segment from ATG to mid S5 was amplified with the primers *MIRK-F(BamHI)* and *MIRK-S1-R*, using *MIRK* cDNA as the template. The second PCR was run again with the same matrix while using primers *MIRK-S2-F* and *MIRK-R(NotI)*, to obtain the cDNA segment *MIRK-S2* from mid S6 to end. The third PCR product *KAT2-S5PS6* segment from S5 to S6 was obtained with the *AtKAT2* plasmid as the template and with the primers *AtKAT2-S5PS6-F* and *AtKAT2-S5PS6-R*. Finally, the chimera *MIRK* mutant gene (*MIRK-By-ΔAtKAT2*) was obtained by PCR, using three cDNA segments *MIRK-S1*, *KAT2-S5PS6* and *MIRK-S2* mixture as the template, with the forward primer *MIRK-F(BamHI)* and the reverse primer *MIRK-R(NotI)*. Thereafter, *MIRK-By-ΔAtKAT2* was inserted to the expression vector pGEM-Xho (at the enzyme restriction sites *BamHI* and *NotI*). Using the same method, the chimera gene *AtKAT2-By-ΔMIRK* was obtained and cloned in pGEM-Xho at the enzyme restriction sites *BamHI* and

NotI.

Expression in *Xenopus* oocytes

CsKAT2 and *CIKAT2* cDNA were integrated into the pGEMXho vector (adapted from pGEMDG vector, D. Becker, Würzburg, Germany) under the control of the T7 promoter between the 5' and 3' untranslated regions of the *Xenopus beta-globin* gene, using the enzyme restriction sites *BamHI* and *NotI* for *CsKAT2*, and *BamHI* and *EcoRI* for *CIKAT2*.

Capped and polyadenylated cRNA of the different studied channels cloned in pGEMXho or pGEMDG (*CsKAT2*, *CIKAT2*, *AtKAT2*, *MIRK*, *MIRK-By-ΔAtKAT2* chimera and *AtKAT2-By-ΔMIRK* chimera) were synthesized in vitro using the mMESSAGE mMACHINE kit (Ambion, Texas, USA).

Oocytes were prepared as previously described by Véry et al. (1995). For *CsKAT2*, *CIKAT2*, *MIRK* or *AtKAT2-By-ΔMIRK* chimera, each oocyte was injected with 30 ng of cRNA or same volume of deionized water (control oocytes). For *KAT2* and *MIRK-By-ΔAtKAT2* chimera, oocytes were injected with 20 ng of cRNA or same volume of deionized water (control oocytes). Then, oocytes were kept at 20°C in 'ND96' solution (96 mM NaCl, 2 mM KCl, 1.8 mM CaCl₂, 1 mM MgCl₂, 2.5 mM Na-pyruvate and 5 mM HEPES-NaOH (pH 7.5)), supplemented with 0.5 mg l⁻¹ gentamycin. Each day, conservation solution was refreshed with new 'ND96' solution to maintain a good living condition for oocytes.

Two-electrode voltage clamp experiments

Two to four days after injection, whole-cell currents were measured using the two electrode voltage-clamp technique using a GeneClamp 500B amplifier (Axon Instruments, Foster City, CA, USA). Voltage-pulse protocols, data acquisition and data analyses were performed using pClamp 9 (Axon Instruments, Foster City, CA, USA) and Sigmaplot 8 software (Jandel Scientific, Erkrath, Germany). All electrodes were filled with 3M KCl. Both actual imposed membrane potential and current were recorded. A correction was made for the voltage drop occurring through the series resistance of the bath and the reference electrode by using two external voltage-measuring electrodes connected to a bath probe (VG-2A-X100 Virtual ground bath clamp; Axon Instruments). Except in the pH sensitivity experiments, all the other measurements were performed in the background solution containing 1.8 mM CaCl₂, 2 mM MgCl₂ and 10 mM Mes / Tris (pH 6.0). Monovalent cations were added as chloride salts. For pH experiment, the background solution contained 1.8 mM CaCl₂, 2 mM MgCl₂ and either 10 mM Mes / Tris when the pH was 5 or 6, or 10 mM HEPES-Tris when the pH was

7.5.

Hydroponic cultivation of cucurbit plants

The seeds of melon (*Cucumis melo* L.), water melon (*Citrullus lanatus*) and cucumber (*Cucumis sativus*) were firstly sanitized and spread on filter papers. After the emerging of radicles and plumules, the seedlings were transferred in plug containing a mixture of peat, perlite and slag (1:1:1 v/v/v) in a plastic greenhouse. When plants were at the 2-3 leaf stage, seedlings were shifted to the hydroponic containers. The nutrient solution used for hydroponic culture contained 413 mg/L $\text{Ca}(\text{NO}_3)_2 \cdot \text{H}_2\text{O}$, 303.5 mg/L KNO_3 , 76.5 mg/L $\text{NH}_4\text{H}_2\text{PO}_4$, 185 mg/L $\text{MgSO}_4 \cdot 7\text{H}_2\text{O}$, 13.9 mg/L $\text{EDTA} \cdot 2\text{Na}$, 18.6 mg/L $\text{FeSO}_4 \cdot 7\text{H}_2\text{O}$, 1.43 mg/L H_3BO_3 , 1.07 mg/L $\text{MnSO}_4 \cdot 4\text{H}_2\text{O}$, 0.11 mg/L $\text{ZnSO}_4 \cdot 7\text{H}_2\text{O}$, 0.04 mg/L $\text{CuSO}_4 \cdot 5\text{H}_2\text{O}$ and 0.01 mg/L $(\text{NH}_4)_2\text{MO}_7\text{O}_{24} \cdot 4\text{H}_2\text{O}$. NaCl was applied to a final concentration of 100 mmol/L. It was gradually increased from 25 mmol/L to 100 mmol/L (25 mM NaCl was added daily until a final concentration of 100 mM was obtained).

Quantitative RT-PCR

Total RNA was extracted from roots, stems, leaves and guard cells of Cucurbitaceae plants using the RNAPrep Pure Plant Kit (TIANGEN, DP432). RNA concentrations were determined using the NanoDrop 1000 Spectrophotometer (Thermo Scientific, USA). Bio protocol for isolation of guard-cell enriched tissues refers to the Jalakas method (Jalakas et al., 2017), and 210-mesh nylon mesh (A. Hartenstein, laborversand.de, catalog number: PAS1) was used to extract pure guard cells. Quantitative real-time PCR reactions were performed with SYBR Green mix (Takara, Japan, RR402A) on Eppendorf Mastercycler ep Realplex (Eppendorf, Germany). The thermal profile was 30 s at 95°C, followed by 40 cycles of 5 s at 95°C, 15 s at 60°C and 15 s at 72°C. The special primers were used for quantitative real-time PCR (Table S1). The quality of the PCR reactions was estimated based on melting curves. Data were analyzed using CFX Manager software. Each qRT-PCR was based on three biological replicates and three technical replicates.

Homology modeling

The protein sequences of the monomers from AtKAT2 (NP_193563.3, *Arabidopsis thaliana*) and MIRK (AAZ66349.2, *Cucumis melo*) were modelled using the I-TASSER server (<http://zhanglab.ccmb.med.umich.edu/I-TASSER/>) (Yang et al., 2015) with default settings. Based on the confidence score (C-score) assigned to the top 5 models by I-TASSER, the best scored model was used for downstream analysis.

The cryo-EM structure of AtKAT1 (Clark et al., 2020), was the template in a structure-based alignment using the MatchMaker tool in UCSF Chimera (Pettersen et al., 2004). Briefly, each of the four chains in the 7CAL structure were aligned to a modelled monomer of the query protein to construct a tetrameric pore using the BLOSUM-62 matrix. The electrostatic potential calculated with Coulomb's law was computed and visualized using Coulombic in UCSF Chimera with Amber20. Color scale was set to ± 3 kcal/(mol \cdot e).

ACCEPTED MANUSCRIPT

Data Availability Statements

The data underlying this article are available in the article and in its online supplementary material.

Funding

This work was supported by the National Natural Science Foundation of China (31372079), State Scholarship Fund of China Scholarship Council (No. 201208310510).

Conflicts of interest

No conflicts of interest declared.

Acknowledgement

We are grateful to Dr. Gareth Steed from the University of Cambridge for his critical reading. We also thank Dr. Ruth Le Fevre for language polishing.

ACCEPTED MANUSCRIPT

References

- Altunlu, H., Gül, A. and Tunc, A. (1997) Effects of nitrogen and potassium nutrition on plant growth, yield and fruit quality of cucumbers grown in perlite. In: International Symposium Greenhouse Management for Better Yield & Quality in Mild Winter Climates 491: 377-382.
- Ardie, S.W., Liu, S. and Takano, T. (2010) Expression of the AKT1-type K⁺ channel gene from *Puccinellia tenuiflora*, PutAKT1, enhances salt tolerance in *Arabidopsis*. *Plant cell reports* 29 (8): 865-874.
- Asch, F., Dingkuhn, M., Dörffling, K. and Miezan K. (2000) Leaf K/Na ratio predicts salinity induced yield loss in irrigated rice. *Euphytica* 113 (2): 109-118.
- Benito, B., Haro, R., Amtmann, A., Cuin, T.A. and Dreyer I. (2014) The twins K⁺ and Na⁺ in plants. *Journal of Plant Physiology* 171(9): 723-731.
- Bhandal, I.S. and Malik, C. (1988) Potassium estimation, uptake, and its role in the physiology and metabolism of flowering plants. *International Review of Cytology* 110: 205-254.
- Boscari, A., Clement, M., Volkov, V., Golldack, D., Hybiak, J., Miller, A.J. et al. (2009) Potassium channels in barley: cloning, functional characterization and expression analyses in relation to leaf growth and development. *Plant, cell and environment* 32 (12): 1761-1777.
- Chakraborty, K., Bose, J., Shabala, L., and Shabala, S. (2016) Difference in root K⁺ retention ability and reduced sensitivity of K⁺-permeable channels to reactive oxygen species confer differential salt tolerance in three Brassica species. *Journal of Experimental Botany* 67(15):4611-4625.
- Clark, M. D., Contreras, G. F., Shen, R., and Perozo, E. (2020) Electromechanical coupling in the hyperpolarization-activated K⁺ channel KAT1. *Nature* 583 (7814), 145-149.
- Demidchik, V. (2014) Mechanisms and physiological roles of K⁺ efflux from root cells. *Journal of Plant Physiology* 171: 696-707.
- Duan, H.R., Ma, Q., Zhang, J.L., Hu, J., Bao, A.K., Wei, L. et al. (2015) The inward-rectifying K⁺ channel SsAKT1 is a candidate involved in K⁺ uptake in the halophyte *Suaeda salsa* under saline condition. *Plant and Soil* 395: 173-187.
- Escalante-Pérez, M., Lautner, S., Nehls, U., Selle, A., Teuber, M., Schnitzler, J.P. et al. (2009) Salt stress affects xylem differentiation of grey poplar (*Populus× canescens*). *Planta* 229 (2): 299-309.
- Fuchs, I., Stölzle, S., Ivashikina, N. and Hedrich, R. (2005) Rice K⁺ uptake channel OsAKT1 is sensitive to salt stress. *Planta* 221 (2): 212-221.

- Gislerød, H. and Adams, P. (1983) Diurnal variations in the oxygen content and acid requirement of recirculating nutrient solutions and in the uptake of water and potassium by cucumber and tomato plants. *Scientia Horticulturae* 21 (4): 311-321.
- Golldack, D., Quigley, F., Michalowski, C.B., Kamasani, U.R. and Bohnert, H.J. (2003) Salinity stress-tolerant and-sensitive rice (*Oryza sativa* L.) regulate AKT1-type potassium channel transcripts differently. *Plant molecular biology* 51 (1): 71-81.
- Handing KB, Niedzialkowska E, Shabalin IG, Kuhn ML, Zheng H and Minor W. (2018) Characterizing metal-binding sites in proteins with X-ray crystallography. *Nature protocols* 13 (5): 1062-1090.
- Hoth, S. and Hedrich, R. (1999) Distinct molecular bases for pH sensitivity of the guard cell K⁺ channels KST1 and KAT1. *Journal of Biological Chemistry* 274 (17): 11599-11603.
- Jeanguenin, L., Alcon, C., Duby, G., Boeglin, M., Chérel, I., Gaillard, I. et al. (2011) AtKC1 is a general modulator of *Arabidopsis* inward Shaker channel activity. *The Plant Journal* 67 (4): 570-582.
- Jeffrey, C. (1980) A review of the Cucurbitaceae. *Botanical Journal of the Linnean society* 81(3): 233-247.
- Jalakas, P., Yarmolinsky, D., Kollist, H. and Brosche, M. (2017). Isolation of Guard-cell Enriched Tissue for RNA Extraction. *Bio-protocol* 7(15): e2447. DOI: [10.21769/BioProtoc.2447](https://doi.org/10.21769/BioProtoc.2447).
- Kaddour, R., Nasri, N., M'rah, S., Berthomieu, P. and Lachaâl, M. (2009) Comparative effect of potassium on K and Na uptake and transport in two accessions of *Arabidopsis thaliana* during salinity stress. *Comptes rendus biologiques* 332 (9):784-794.
- Kaya, C., Kirnak, H. and Higgs, D. (2001) Effects of supplementary potassium and phosphorus on physiological development and mineral nutrition of cucumber and pepper cultivars grown at high salinity (NaCl). *Journal of Plant Nutrition* 24 (9): 1457-1471.
- Kourie, J. and Goldsmith, M.H.M. (1992) K⁺ channels are responsible for an inwardly rectifying current in the plasma membrane of mesophyll protoplasts of *Avena sativa*. *Plant Physiology* 98 (3): 1087-1097.
- Kronzucker, H.J. and Britto, D.T. (2011) Sodium transport in plants: a critical review. *New Phytologist* 89(1): 54-81.
- Lebaudy, A., Vavasseur, A., Hosity, E., Dreyer, I., Leonhardt, N., Thibaud, J.-B., Véry, A.-A., Simonneau, T. and Sentenac, H. (2008). Plant adaptation to fluctuating environment and biomass production are strongly dependent on guard cell potassium channels. *Proceedings of the National*

- Academy of Sciences USA* 105: 5271–5276.
- Maathuis, F.J. (2006) The role of monovalent cation transporters in plant responses to salinity. *Journal of Experimental Botany* 57 (5): 1137-1147.
- Munns, R. and Tester, M. (2008). Mechanisms of salinity tolerance. *Annual Review of Plant Biology* 59: 651–681.
- Obata, T., Kitamoto, H.K., Nakamura, A., Fukuda, A. and Tanaka Y. (2007) Rice shaker potassium channel OsKAT1 confers tolerance to salinity stress on yeast and rice cells. *Plant physiology* 144 (4): 1978-1985.
- Pettersen, Eric F., Thomas D. Goddard, Conrad C. Huang, Gregory S. Couch, Daniel M. Greenblatt, Elaine C. Meng, and Thomas E. Ferrin. (2004) UCSF Chimera—a visualization system for exploratory research and analysis. *Journal of computational chemistry* 25 (13): 1605-1612.
- Pilot, G., Gaymard, F., Mouline, K., Chérel, I. and Sentenac, H. (2003a) Regulated expression of *Arabidopsis* Shaker K⁺ channel genes involved in K⁺ uptake and distribution in the plant. *Plant molecular biology* 51 (5): 773-787.
- Pilot, G., Pratelli, R., Gaymard, F., Meyer, Y. and Sentenac, H. (2003b) Five-group distribution of the Shaker-like K⁺ channel family in higher plants. *Journal of Molecular Evolution* 56: 418–434.
- Pitrat, M. (2008) Melon. In: Prohens J., Nuez F. (eds) Vegetables I. Handbook of Plant Breeding, vol 1. Springer, New York, NY.
- Robinson, M.F., Véry, A.-A., Sanders, D. and Mansfield, T.A. (1997). How can stomata contribute to salt tolerance? *Annals of Botany* 80: 387–393.
- Serrano, R. (1996) Salt tolerance in plants and microorganisms: toxicity targets and defense responses. *International review of cytology* 165: 1-52.
- Su, H., Gollack, D., Katsuhara, M., Zhao, C. and Bohnert, H.J. (2001) Expression and stress-dependent induction of potassium channel transcripts in the common ice plant. *Plant Physiology* 125 (2): 604-614.
- Su, Y.H., North, H., Grignon, C., Thibaud, J.B., Sentenac, H. and Véry, A.A. (2005) Regulation by external K⁺ in a maize inward Shaker channel targets transport activity in the high concentration range. *The Plant Cell* 17 (5): 1532-1548.
- Tester, M. and Davenport, R. (2003) Na⁺ tolerance and Na⁺ transport in higher plants. *Annals of botany* 91 (5): 503-527.

- Véry, A.A., Gaymard, F., Bosseux, C., Sentenac, H. and Thibaud, J.B. (1995) Expression of a cloned plant K⁺ channel in *Xenopus* oocytes: analysis of macroscopic currents. *The Plant Journal* 7 (2): 321-332.
- Véry, A.A., Nieves-Cordones, M., Daly, M., Khan, I., Fizames, C. and Sentenac, H. (2014) Molecular biology of K⁺ transport across the plant cell membrane: what do we learn from comparison between plant species? *Journal of Plant Physiology* 171:748-769.
- Véry, A.A., Robinson, M.F., Mansfield, T.A. and Sanders, D. (1998) Guard cell cation channels are involved in Na⁺-induced stomatal closure in a halophyte. *The Plant Journal* 14 (5): 509-521.
- Wang, L.M., Véry, A.A., Zhang, Y.D., Deng, Y.W. and Huang, D.F. (2011) Search for Molecular Bases of Salt Blockage in MIRK of Melon in *Xenopus* Oocytes. *Plant Physiology Journal* 47 (2): 193~198 (in chinese).
- Wang, L.M., Wei, S.W., Chen, J.B., Zhang, Y.D. and Huang, D.F. (2013) Regulation of the inward rectifying K⁺ channel MIRK and ion distribution in two melon cultivars (*Cucumis melo* L.) under NaCl salinity stress. *Acta Physiologiae Plantarum* 35(9): 2789~2800.
- Yang, G., Sentenac, H., Véry, A.A. and Su, Y. (2015) Complex interactions among residues within pore region determine the K⁺ dependence of a KAT1-type potassium channel AmKAT1. *The Plant Journal* 83 (3): 401-412.
- Yang, J., and Zhang, Y. (2015). I-TASSER server: new development for protein structure and function predictions. *Nucleic Acids Res* 43(W1):W174-W181. doi:10.1093/nar/gkv342
- Zhang, Y., Wang, Z., Zhang, L., Cao, Y., Huang, D. and Tang, K. (2006) Molecular cloning and stress-dependent regulation of potassium channel gene in Chinese cabbage (*Brassica rapa* ssp. *Pekinensis*). *Journal of plant physiology* 163 (9):968-978.
- Zhang, Y.D., Véry, A.A., Wang, L.M., Deng, Y.W., Sentenac, H. and Huang, D.F. (2011) A K⁺ channel from salt-tolerant melon inhibited by Na⁺. *New Phytologist* 189 (3): 856-868.
- Zhu, J.K. (2003) Regulation of ion homeostasis under salt stress. *Current opinion in plant biology* 6 (5): 441-445.

Figure legends

Figure 1. Phylogenetic tree of CsKAT2 and ClKAT2 with Shaker channels from other plants.

The multiple alignments were generated using Geneious program. The accession numbers of proteins are as follows: AKT1, AAB95299; SPICK1, AAD16278; TaAKT1, AAF36832; MKT1, AAF81249; KMT1, AAF81250; SIRK, AAL09479; KCT2, AAX19659; MIRK, AAZ66349; AKT6, AECO7722; GORK, AED94198; SKOR, AEE73866; AmKAT1, AKR53708; KST1, CAA56175; SKT1, CAA60016; SKT2, CAA70870; Vfk1, CAA71598; KDC1, CAB62555; PTORK, CAC05488; KPT1, CAC87141; KZM1, CAD18901; AtKC1, NP-194991; AKT2, NP-567651; ZMK2, NP-001105120; ZMK1, NP-001105480; KZM2, CAD90161; KAT1, NP-199436; KAT2, NP-193563.

Figure 2. Characterization of CsKAT2 and ClKAT2 in *Xenopus* oocytes

A-C. Representative current traces of oocytes injected with H₂O (A), 30 ng of *CsKAT2* cRNA (B) or 30 ng of *ClKAT2* cRNA (C) recorded from 30 mV to -180 mV in -15 mV increments, with holding potential at -30 mV or -40 mV and deactivation potential at -20 mV or -30 mV, in 10 mM K⁺ solution.

D. Effect of external K⁺ on *CsKAT2* currents and the corresponding reversal potentials (E_{rev}). Currents were successively recorded in external solutions containing a variable KCl concentration (1, 3, 10 or 100 mM), and a ionic background of 1.8 mM CaCl₂, 2 mM MgCl₂ and 10 mM Mes / Tris (pH 6.0). E_{rev} was plotted as a function of the external potassium concentration. The solid line shows a logarithmic fit to the experimental data.

E. As D but for *ClKAT2*.

F. Affinity of *CsKAT2* (left) and *ClKAT2* (right) to external K⁺. The inward conductance at the different K⁺ concentrations, determined at infinitely negative voltage, was obtained from fits of time-activated currents with a Goldman-Hodgkin-Katz equation coupled with a Boltzmann equation: $I = \{G * E * [1 - \exp(F * (E - E_{rev}) / (R * T))] / [1 - \exp(F * E / (R * T))]\} * \{1 / [1 + \exp(z * F * (E - E_{a50}) / (R * T))]\}$, where I is the steady-state current, G is inward conductance at infinitely negative membrane potential, E is the applied membrane potential, E_{rev} is reversal potential, z is the equivalent gating charge, E_{a50} is half activation potential, F is Faraday's constant, R is perfect gas constant and T is temperature. The solid line represents a Michaelis-Menten fit (Véry et al. 1995).

G. Voltage dependence of *CsKAT2* (left) and *ClKAT2* (right) channel activity. P_o/P_{o,max} was assumed to follow a Boltzmann distribution and was obtained from the fit of the time-activated currents with the Goldman-Hodgkin-Katz equation coupled with the Boltzmann equation (Cf. C and D). The gating charge (z) and half-activation potential (E_{a50}) were given in the figure panels.

H. Current-voltage (I/V) relationships of *CsKAT2* (left) and *ClKAT2* (right) in the presence of different monovalent cations. Currents were recorded in bath solutions containing successively 100 mM of either KCl (K100), RbCl (Rb100), NH₄Cl (NH₄100), LiCl (Li100) or NaCl (Na100), pH 5.5.

I. External pH effect on *CsKAT2* (left) and *ClKAT2* (right) currents. Currents were recorded in 10 mM KCl-containing external solutions at varying pH (5, 6 and 7.5).

Date are means ± SE, n=4-5 in D; n=6-7 in E; n=3-4 for *CsKAT2* and n=6 for *ClKAT2* in F and G; n=9 for *CsKAT2* and n=11 for *ClKAT2* in H; n=4 for *CsKAT2* and n=5 for *ClKAT2* in I.

Figure 3. External Na⁺ blocked CsKAT2 and ClKAT2 currents but not AtKAT2 currents

A-C. Representative CsKAT2 (A), ClKAT2 (B) and AtKAT2 (C) current traces recorded in 1 mM K⁺ and 99 mM of either Li⁺ (-Na) or Na⁺ (+Na) from +30 to -165 mV (A and B) and +40 to -155 mV (C) in -15 mV increments (top panels). The corresponding deactivated currents (dashed circle) were zoomed and showed in the lower panels.

D-F. Mean of steady-state CsKAT2 (D), ClKAT2 (E) and AtKAT2 (F) inward currents against the membrane voltage in the presence of Li⁺ or Na⁺ at the external concentration of 1 mM K⁺ (K1). Data concern time-activated currents and are means ± SE, n=5 in D, E and F.

G. Comparison of the extent of blockage by Na⁺ on MIRK, CsKAT2, ClKAT2 and AtKAT2 inward currents at -155 mV in 1 mM K⁺ and 99 mM Na⁺. Different letters at the right of the bars indicate significant differences (*t* test, P<0.05).

Figure 4. Expression profile of KAT2-like channels in Cucurbitaceae plants.

A. Expression patterns of KAT2-like channels in different tissues of plants. The RNAs were extracted from the roots, stems, leaves, mid rib of leaves and guard cells respectively. *Actin* was used as internal control. Data are presented as means ± SD from three biological repeats.

B. Expression profile of KAT2-like channel genes in Cucurbitaceae plants after 24 h under NaCl treatment. KAT2-like channel gene transcript levels were detected by qRT-PCR 24 h after plant treatment by addition of 100 mM NaCl. Data were shown as means ± SD from three biological repeats. The significance level was defined as * (P < 0.05), ** (P < 0.01).

Figure 5. The inhibition by Na⁺ was abolished in MIRK-By-ΔAtKAT2 channel, and appeared in AtKAT2-By-ΔMIRK channel.

A. Amino acid sequence alignment of MIRK and KAT2 transmembrane segments (S1 to S6). The portion of MIRK amino acid sequence between the two inverted triangles was replaced by the corresponding sequence of KAT2 in the chimera named MIRK-By-ΔAtKAT2. The reciprocal chimera was named AtKAT2-By-ΔMIRK.

B. Example of MIRK-By-ΔAtKAT2 current traces recorded in 1 mM external K⁺ and 99 mM of either Li⁺ (upper panel) or Na⁺ (lower panel). The membrane was clamped from -15 mV to -165 mV by step of -15 mV. The corresponding deactivation currents recorded upon return to the holding potential at -15 mV in both solutions were zoomed at the right.

C. Inward current-voltage relationship of MIRK-By-ΔAtKAT2 in the presence of Li⁺ or Na⁺ at 1 mM K⁺.

D. Example of AtKAT2-By-ΔMIRK current traces recorded in 1 mM external K⁺ and 99 mM of either Li⁺ (upper panel) or Na⁺ (lower panel). The membrane was clamped from +15 mV to -165 mV by step of -15 mV. The corresponding deactivation currents recorded upon return to the holding potential at -40mV in both solutions were zoomed at the right.

E. Same as C but for AtKAT2-By-ΔMIRK channel.

Data concern time-activated currents and are means ± SE (n=9 in both C and E).

Figure 6. Modeling and comparison of the electrostatic map of AtKAT2 and MIRK.

A. Ribbon diagrams of AtKAT2 and MIRK channels composed from 4-subunits. Red sections of the ribbon diagram indicate the P domain-motif, and blue coloured sections represent the residues from the S5 to S5-P linker (from N222 to S260 in MIRK; corresponding to the residues A216 to S254 in AtKAT2).

B. Electrostatic potential distribution representation from the top view of AtKAT2 and MIRK. Negatively charged surface is indicated in red and positively charged in blue. Blue sections in the ribbon diagram from A, were highlighted in green and arrows point to the pore structure. Electrostatic potential range is $-3kT/e$ (red) to $+3kT/e$ (blue).

C. Close-up of S5 to S5-P-linker side view of AtKAT2 and MIRK. Green highlighted areas from B are shown for reference.

D. Cartoon diagram of AtKAT2 and MIRK with arrows pointing to key residues outside the pore. Key residues are showed in electrostatic potential surface and highlighted in green. Same color bar scale in AtKAT2 as MIRK.

Figure 1

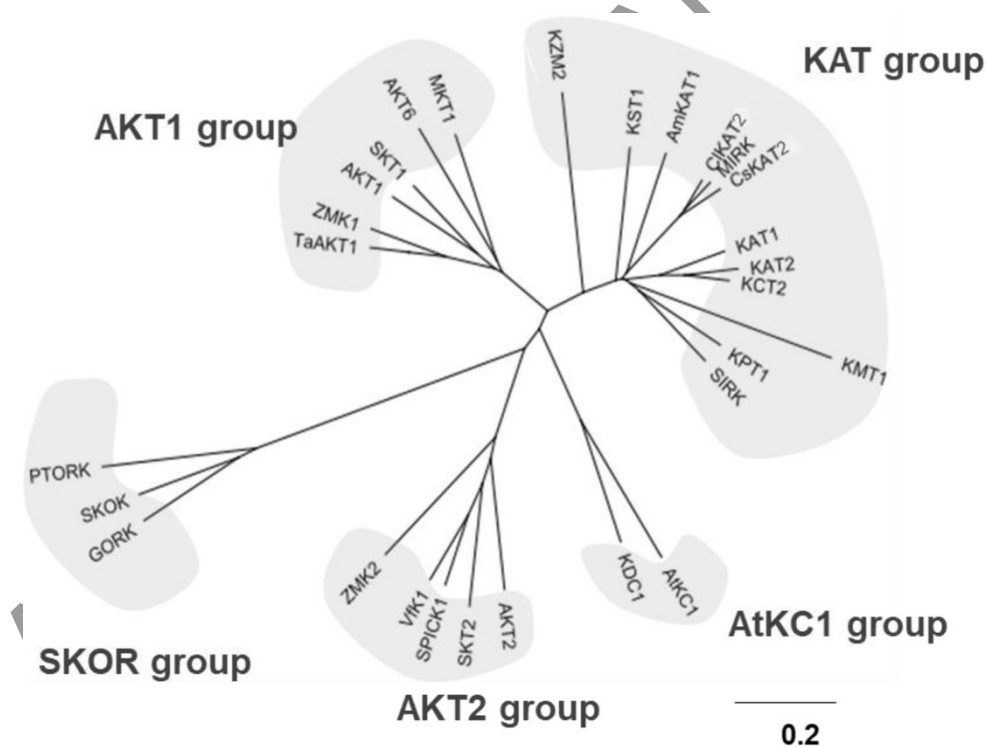


Fig 1

Figure 2

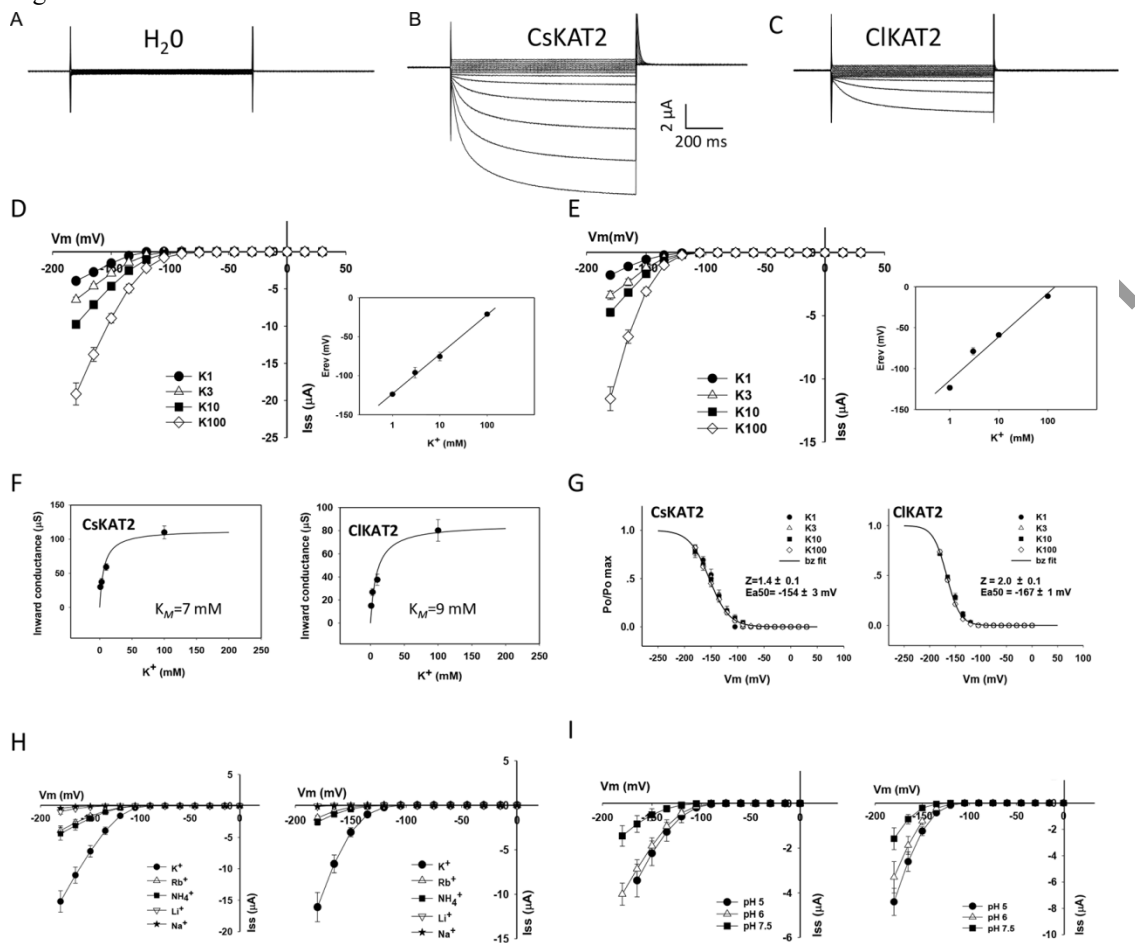
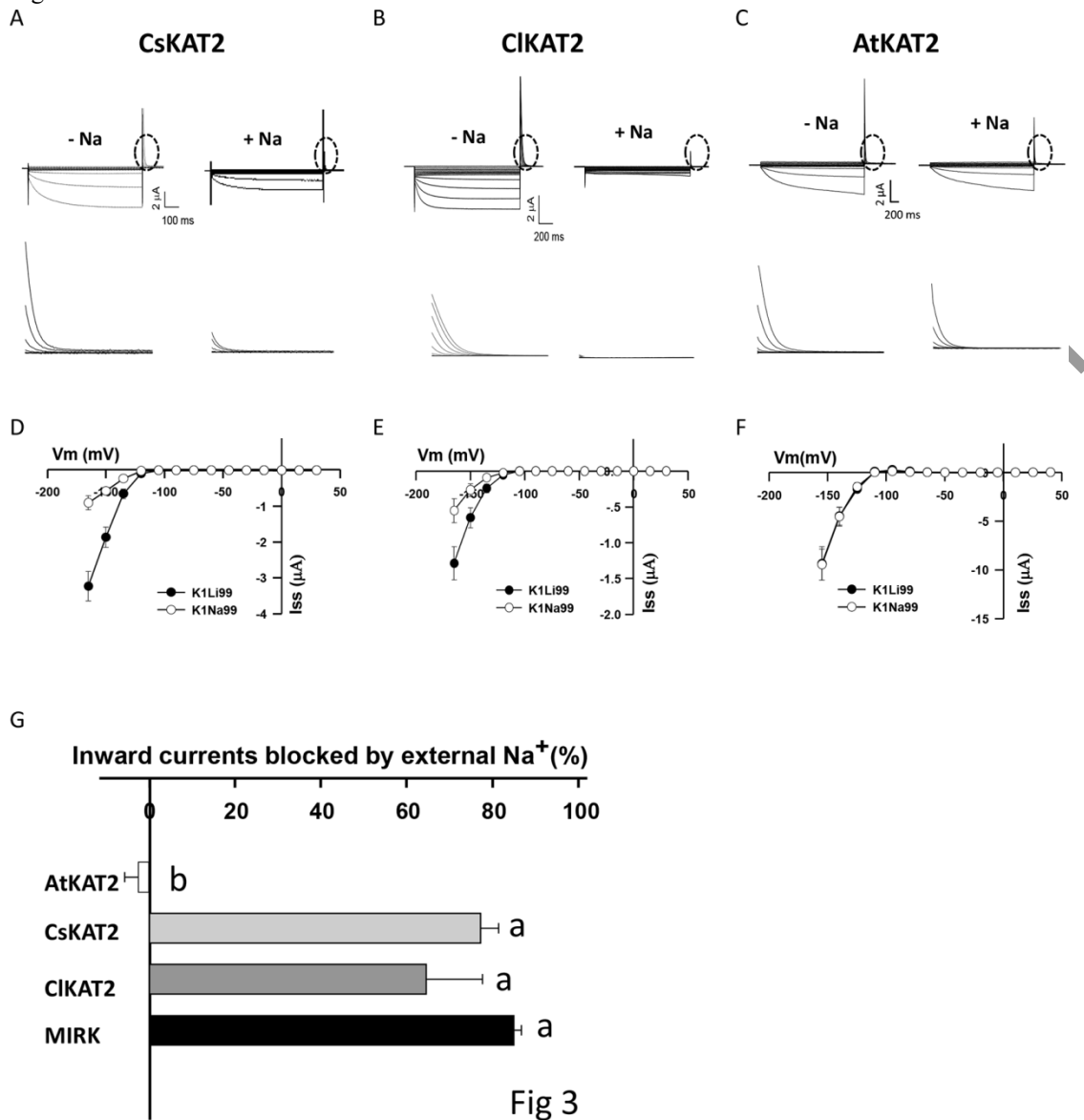


Fig 2

ACCEP

Figure 3



ACCEPT

Figure 4

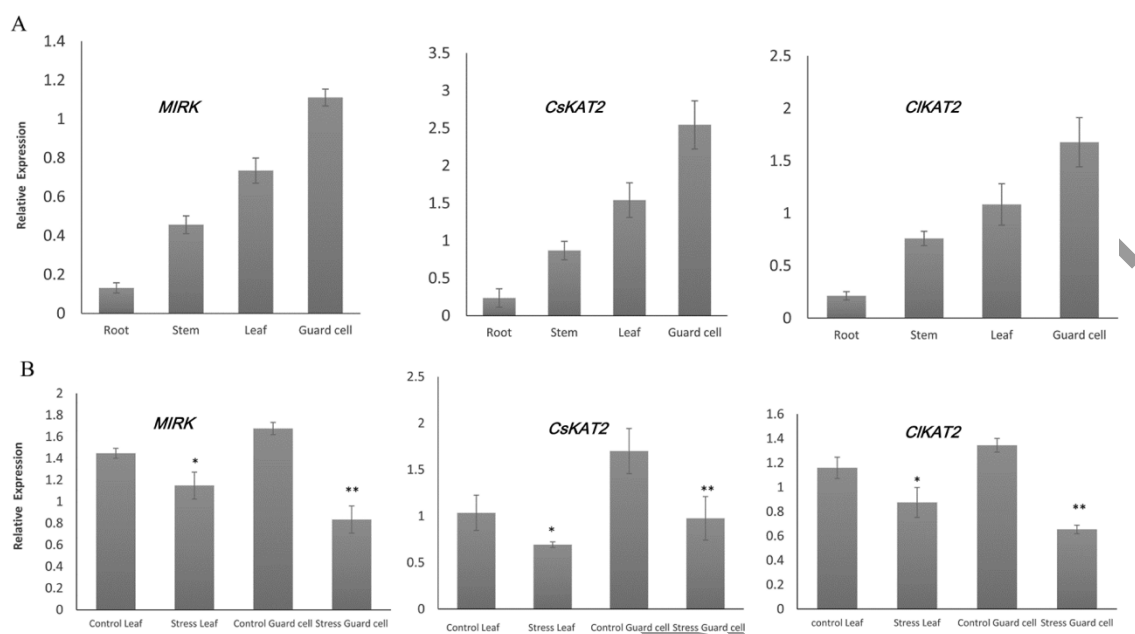


Figure 5
A

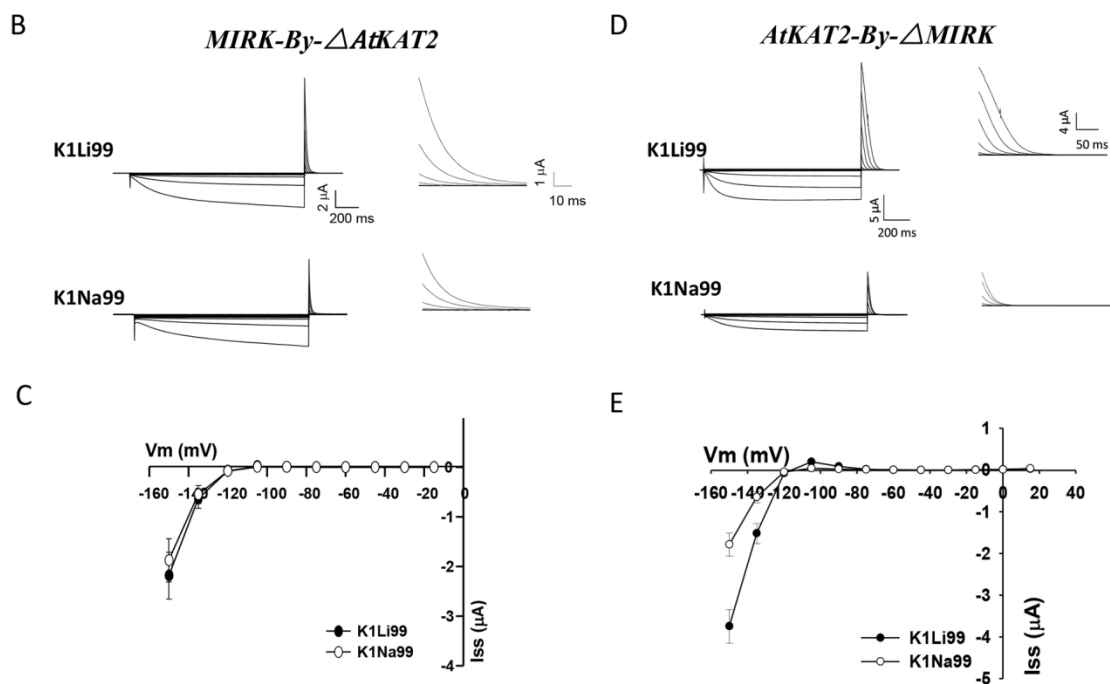
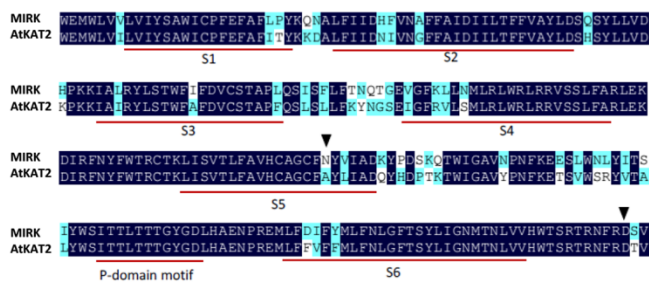


Fig 5

ACCEPT

Figure 6

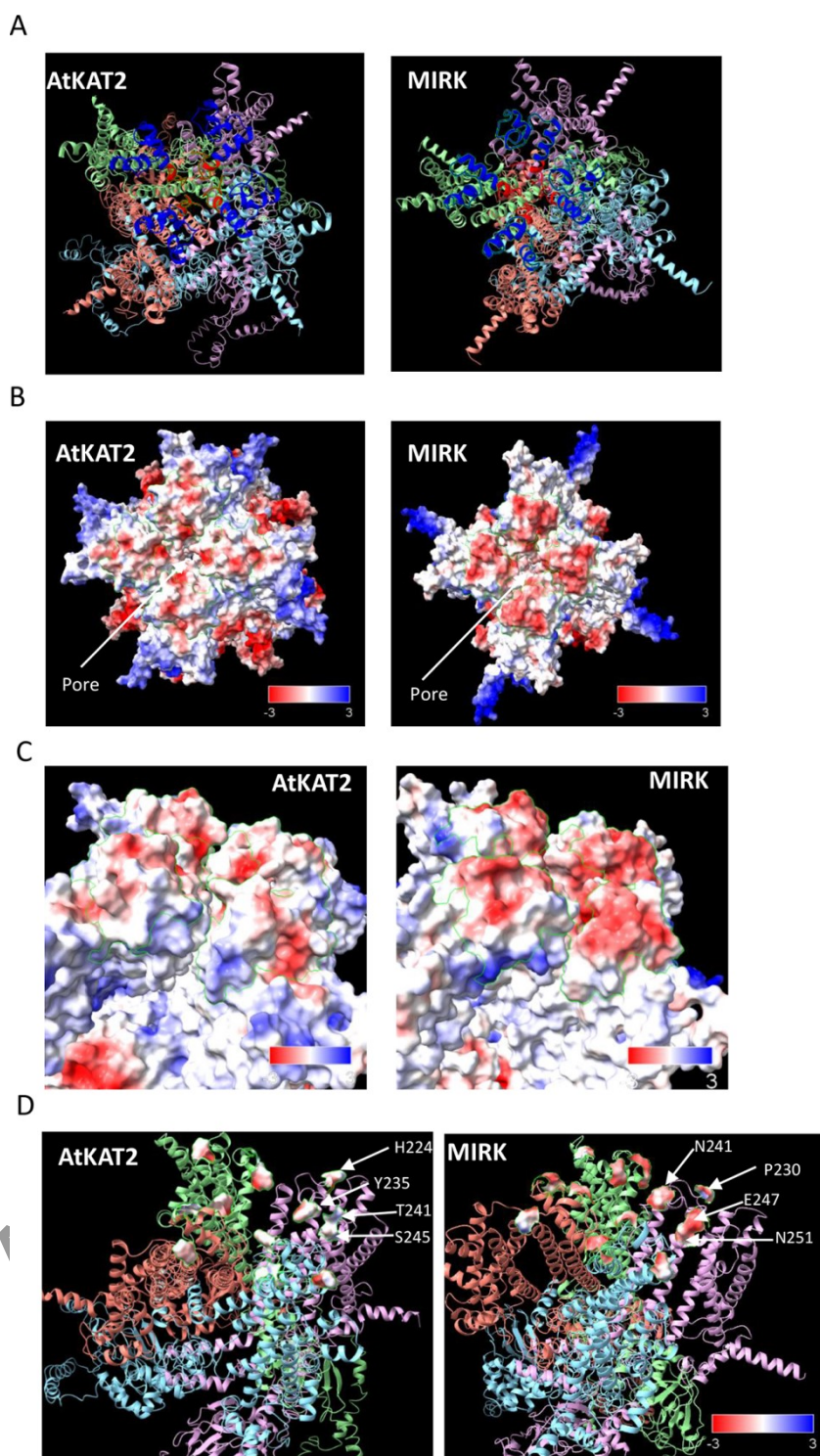


Fig 6

SCRIPT